SIMVASTATIN INHIBITS CENTRAL SYMPATHETIC OUTFLOW IN HEART FAILURE BY A NOS MECHANISM

Lie Gao, **Wei Wang**, and **Irving H. Zucker**
Department of Cellular and Integrative Physiology (L.G., W.W., I.H.Z.)

Abstract

Our previous study demonstrated that oral treatment with simvastatin (SIM) suppressed renal sympathetic nerve activity (RSNA) in the rabbits with chronic heart failure (CHF). The purpose of this experiment was to determine the effects of direct application of SIM to the central nervous system on RSNA and its relevant mechanisms. Experiments were carried out on 21 male New Zealand White rabbits with pacing induced CHF. The CHF rabbits received infusion of vehicle, SIM, or SIM + L-NAME into the lateral cerebral ventricle via osmotic minipump for 7 days. We found that, (1) In CHF rabbits, icv infusion of SIM significantly suppressed basal RSNA (1st day 69.5 ± 8.9 % of Max; 7th day 26.0 ± 6.0 % of Max. $P < 0.05$, n = 7) and enhanced arterial baroreflex function starting from the 2nd day and lasting through the following 5 days; (2) Statin treatment significantly upregulated nNOS protein expression in the rostral ventrolateral medulla (RVLM) (Control, n = 6, 0.12 ± 0.04; SIM treated, n = 7, 0.31 ± 0.05. $P < 0.05$); (3) In CATH.a neurons, incubation with SIM significantly upregulated the nNOS mRNA expression, which was blocked by co-incubation with Mevalonate, farnesyl-pyrophosphate, or geranylgeranyl-pyrophosphate; (4) Incubation with Y-27632 significantly upregulated nNOS mRNA expression in these neurons. These results suggest that central treatment with SIM decreased sympathetic outflow in CHF rabbits via up regulation of nNOS expression in RVLM, which may be due to the inhibition of HMG-CoA reductase and a decrease in Rho Kinase by SIM.

Introduction

Chronic heart failure (CHF) is characterized by both sympatho-excitation(Packer, 1992) and blunted arterial baroreflex function(DiBona and Sawin, 1995). Our previous studies demonstrated that oral treatment with the HMG-CoA (3-hydroxy-3-methylglutaryl coenzyme A) reductase inhibitor, simvastatin (SIM), improved baroreflex function and normalized sympathetic outflow in the rabbits with CHF(Pliquett, et al., 2003). In previous experiments we have demonstrated that these therapeutic effects of SIM correlated with changes in several important signaling molecules in the rostral ventrolateral medulla (RVLM) of rabbits with CHF (Gao, et al., 2005a). These experiments were based on systemic (oral) administration of SIM. Therefore it is difficult to determine if these effects were mediated by central or peripheral mechanisms following oral administration of SIM. Because SIM has been demonstrated to permeate the blood-brain barrier(Saheki, et al., 1994), we therefore postulated that the above effects of oral SIM were mediated, at least partially, by central mechanisms. Our first hypothesis in the current experiment was that direct administration of SIM into the brain will reduce sympathetic nerve activity in the CHF state.

Corresponding Author: LIE GAO, MD, Ph.D., Department of Cellular and Integrative Physiology, University of Nebraska Medical Center, 985850 Nebraska Medical Center, Omaha, Nebraska 68198-5850, Tel: (402) 559 8491, FAX: (402) 559 4438, Email: lgao@unmc.edu.

There is considerable evidence suggesting that nitric oxide (NO) in the central nervous system, especially in the brainstem, plays an important role in the regulation of sympathetic outflow and blood pressure (Zanzinger, 1999; Krukoff, 1999). The RVLM is the last relay station in the brain to integrate sympathetic outflow(Dampney, 1994). The sympathetic premotor neurons of the RVLM provide the major tonic excitatory input to sympathetic preganglionic neurons in the spinal cord (Guertzenstein and Silver, 1974). Chan et al.(Chan, et al., 2001; Chan, et al., 2003) have demonstrated the existence of nitric oxide synthase (NOS) in the RVLM. On the other hand, Bredt et al. (Bredt, et al., 1990) demonstrated that NO synthase in the brain to be exclusively associated with discrete neuronal populations. Treatment with a precursor of NO(Shapoval, et al., 1991) or an NO donor(Kagiyama, et al., 1997) into the RVLM caused a marked depressor response. In contrast, NOS inhibitors were found to cause a pressor response in anesthetized animals (Tseng, et al., 1996).

Interestingly, Hirooka et al.(Hirooka, et al., 2003) reported that reduced nNOS expression in the RVLM, and the resulting reduction of NO production contributed to the enhanced sympathetic drive in CHF rats. Using the same animal model, we found that delivery of Ad.nNOS into the RVLM to increase nNOS expression and NO production normalized sympathetic outflow and enhanced arterial baroreflex function(Wang, et al., 2003). In spontaneously hypertensive rats, another animal model characterized by sympatho-excitation, increased NO production caused by the overexpression of eNOS in the RVLM led to an increase in the maximum gain of the baroreflex control of HR(Kishi, et al., 2003) and a decrease in mean arterial pressure (MAP), heart rate (HR), sympathetic nerve activity, and 24 hour urinary norepinephrine excretion(Kishi, et al., 2002).

On the other hand, recent animal experiments have demonstrated the up regulation of activity and expression for iNOS(Ye, et al., 2006), eNOS(Di Napoli, et al., 2001), and nNOS(Nakata, et al., 2007) by statins. Our second hypothesis in the current experiments therefore is that, in the rabbit with CHF, SIM normalizes sympathetic outflow via a central nNOS-NO mechanism. The primary goals of this experiment were to determine the effect of chronic icv infusion of SIM on renal sympathetic nerve activity (RSNA), arterial baroreflex function, and nNOS protein expression in the RVLM of CHF rabbits. In addition, we also explored the pathway mediating the SIM induced nNOS expression using a neuronal cell culture.

Methods

Animals

Experiments were carried out on 21 male New Zealand White rabbits weighing between 3.3 and 4.2 kg. These experiments were reviewed and approved by the University of Nebraska Medical Center Institutional Animal Care and Use Committee and conformed to the *Guidelines for the Care and Use of Experimental Animals* of the American Physiological Society and the National Institutes of Health. Rabbits were assigned to one of 3 groups; a control group (treated with intracerebroventricular (icv) artificial CSF as vehicle, n = 6), a SIM group (n = 7), a SIM plus L-NAME group (n = 5). These rabbits received infusions for 7 days, the basal RSNA and baroreflex function were measured daily, and nNOS protein expression in the RVLM was determined after 7 days of icv infusion. We also used another 4 CHF rabbits to determine nNOS protein expression in the RVLM after 2 days of icv infusion of SIM.

Induction of CHF

CHF was induced by chronic ventricular tachycardia for 3–4 weeks, as previously described (Pliquett, et al., 2003). Heart failure was characterized by a minimum of a 50% reduction in baseline ejection fraction compared with the pre paced state, a 2 mm dilation of the left ventricle

in both systole and diastole, and by clinical signs of CHF, such as pleural fluid, ascites, pulmonary congestion, and cachexia.

Chronic lateral cerebral ventricle infusion

All rabbits received an implantation of a 19 gauge cannula into the lateral cerebral ventricle as previously described(Gao, et al., 2005b). An osmotic mini pump (model 2001, DURECT Corporation, Cupertino, CA) filled with artificial (a)CSF, SIM (5μg/0.5μl/h), or SIM (5μg/0.5μl/h) + L-NAME (50μg/0.5μl/h) was implanted subcutaneously in the back of neck and connected to the cerebroventricular cannula. At the end of each experiment, the placement of the cannula was confirmed by injection of 50 μl 2% Pontamine Sky Blue into the lateral cerebral ventricle via the cannula.

Arterial pressure, heart rate, and renal sympathetic nerve recording

A catheter connected to a radio-telemetry unit (Data Sciences International, St. Paul, Mn) was inserted into the descending aorta via a branch of the right femoral artery for direct measurement of arterial pressure (AP). Heart rate (HR) was derived from the AP pulse using a PowerLab (Model 8S; AD Instruments Inc., Colorado Springs, CO) data acquisition system. Renal sympathetic nerve recording was carried out in the conscious state as described previously(Liu and Zucker, 1999).

Evaluation of arterial baroreflex function

AP, HR and RSNA were recorded on a Powerlab system. An intravenous infusion of sodium nitroprusside (NP) and then phenylephrine (PE) was used to induce alterations of AP. Baroreflex sensitivity was expressed as the slope of the linear regression relating changes in integrative RSNA to changes in MAP from the lowest AP induced by NP to the peak pressure induced by PE.

Preparation of RVLM tissue

At the end of experiment, the rabbits were euthanized with pentobarbital sodium. The brain was removed and immediately frozen on dry ice, blocked in the coronal plane and sectioned at 150 μm thickness in a cryostat. The bilateral RVLM areas (2.0 to 3.5 mm from the obex, 2.5 to 4.0 mm from middle line, and within the ventrolateral area of section) were punched out using a 15-gauge needle stub (ID 1.5 mm) for the analysis of protein of nNOS.

Western Blot Analysis for nNOS

Protein from RVLM of rabbits was extracted using RIPA buffer, the concentration of which was then measured using a protein assay kit (Pierce; Rockford, IL) and was adjusted to the same with equal volumes of 2X 4% SDS sample buffer. The samples were then boiled for 5 min following by loading on the 7.5% SDS-PAGE gel (5 μg protein/30 μL per well) for electrophoresis using Bio-Rad mini gel apparatus at 40 mA/each gel for 45 min. Then the fractionized proteins on the gel were electrophoretically transferred onto the PVDF membrane (Millipore) at 300 mA for 90 min. The membrane was probed with primary antibody (nNOS mouse lgG2a, BD Biosciences, 1:1000) and secondary antibody (goat anti-mouse IgG-HRP, Santa Cruz, 1:2500), and then treated with enhanced chemi-luminescence substrate (Pierce; Rockford, IL) for 5 min at room temperature. The bands in the membrane were visualized and analyzed using UVP BioImaging Systems.

CATH.a Cell Culture

A neuronal cell line (CATH.a) was purchased from American Type Culture Collection (ATCC, Manassas, VA) and grown in RPMI 1640 containing 8% horse serum, 4% fetal bovine serum,

1% penicillin-streptomycin, at 37□ in a humidified atmosphere equilibrated with 5% CO_2. After subculture, cells were plated on polystyrene tissue culture dishes at a density of 1×10^7 cells/100-mm plate with N 6,2′-O-dibutyryladenosine 3′,5′-cyclemonophosphate (dbcAMP1 mmol/L, Sigma) to grow for 2 days in order to obtain differentiated CATH.a cells and then were treated with SIM alone or plus Mevalonate, Farnesylpyrophosphate (FPP),Geranylgeranylpyrophosphate (GGPP), or Y-27632 for 1–3 days.

Real-time RT-PCR Analysis of nNOS mRNA

Total RNA from CATH.a cell pellets for Real-time RT-PCR was extracted using RNeasy columns (Qiagen; Valencia, CA), which then was reverse transcribed into double-stranded cDNA. Real-time RT-PCR was carried out using the thermocycler (PTC-200 Peltier Thermal Cycler with CHROMO 4 Continuous Fluorescence Detector, BIO-RAD) according to the manufacturer's recommendations. Cycle numbers obtained at the log-linear phase of the reaction were plotted against a standard curve prepared with serially diluted control samples. Expression of target genes was normalized by GAPDH levels. The primers and probes used in this experiment were designed using software on the internet website: https://www.genscript.com/ssl-bin/app/primer, and synthesized in the Eppley Institute Molecular Biology Core Lab on the campus of the University of Nebraska Medical Center. Table 1 shows the gene-specific primers and probes. The primers and probes to detect gene expression in the CATH.a neuron sample were designed according to the mouse gene sequences since these neurons are derived from a transgenic mouse brain locus coeruleus.

Statistical Analysis

Data are expressed as the mean ±SE. The differences between groups were determined with a one way ANOVA followed by the student Newman-Keuls test for analysis of significance. The differences before and after icv infusion in each group were analyzed with a paired t test. Statistical significance was defined as $P < 0.05$.

Results

Body weight, ratio of organ weight to body weight, hemodynamics, and echo data

Table 2 shows the values for body weight, ratio of organ weight to body weight, hemodynamics, and echo data in the CHF rabbits from the three groups studied. Hemodynamics and echo data were measured respectively before and at day 7 post icv infusions of reagents. While only CHF rabbits were studied they exhibited higher ratios of heart and lung weight to body weight, higher LVEDP and LVEDD, and lower EF compared to normal rabbits from previous studies in our laboratory(Gao, et al., 2005a). There were no significant changes in these parameters between the three groups of rabbits studied here.

icv infusion of SIM decreases baseline RSNA

An original recording of AP, HR and RSNA pre- and 7 day post- icv infusion of SIM in conscious CHF rabbits is shown in figure 1. Compared with panel A (before infusion), icv infusion of vehicle (aCSF) did not exhibit any effects on the RSNA (panel B). In contrast, from the panel D, we can clearly see a noticeable decrease in basal RSNA at day 7 after icv infusion of SIM compared with the before SIM infusion (panel C), indicating that central treatment with SIM suppressed sympathetic nerve activity in the CHF state. However, we did not see a marked alteration of blood pressure or heart rate after icv infusion of vehicle, simvastatin, or simvastatin plus L-NAME. Figure 2 is the grouped data illustrating the effects of icv infusion of SIM on basal RSNA in conscious CHF rabbits. From this figure, we can see that icv infusion of SIM caused a decrease in RSNA beginning at day 2 which was sustained up to day 7, compared with either day 0 or vehicle treatment. On the other hand, icv infusion of SIM plus L-NAME,

prevented the sympatho-inhibition of SIM alone. This suggests that the response to SIM was, at least in part, due to an NO mechanism.

icv infusion of SIM improves baroreflex function

Figure 3 illustrates original recordings of AP, HR and RSNA responses before (panels A and C) or after (panels B and D) icv infusion of vehicle (panel A and B) or SIM (panel C and D) in conscious CHF rabbits. The vehicle treated rabbit exhibited a worsening of the baroreflex sympatho-inhibition and bradycardia over time. In contrast, the SIM treated rabbit showed an improvement in baroreflex function over the same time period. Figure 4 shows the mean data for the baroreflex slope for the control for RSNA. The baroreflex slope increased starting at day 2 following SIM treatment compared with the vehicle treatment and from the day 4 compared with day 0 (before SIM treatment). The peak effect of SIM on baroreflex function occurred at day 7 after infusion. In contrast, the baroreflex slope in the CHF rabbits receiving icv infusion of SIM plus L-NAME showed no significant difference from the vehicle treatment.

icv infusion of SIM upregulates nNOS protein expression in the RVLM

Because L-NAME abolished the SIM induced inhibition of RSNA we postulated that NO/NOS was a major mediator of the effect of SIM treatment. nNOS protein expression in the RVLM of CHF rabbits was significantly up regulated after 7 days of icv infusion of SIM. Figure 5 clearly shows an increase in nNOS protein from the RVLM of rabbits receiving the icv infusion of SIM compared to that from the vehicle treated rabbits. Given that SIM decreased basal RSNA and improved the baroreflex function rabbits from day 2 after treatment, we therefore measured the nNOS protein expression in the RVLM of three CHF rabbits following 48 hours icv infusion of SIM. We found that the nNOS protein expression was upregulated after 48 hours of SIM treatment (the Ratio of nNOS to GAPDH: 0.27 ± 0.06 in 48h SIM treatment, n = 3; 0.31 ± 0.05 in 7d SIM treatment, n = 7; 0.12 ± 0.04 in vehicle treatment, n = 6).

It is worthy to note that we also measured nNOS protein expression in the hypothalamus, another sympathetic-related nucleus, in these rabbits. We found higher expression of nNOS protein in this area, but we did not find significant differences between vehicle, SIM, and SIM plus L-NAME treated rabbits. On the other hand, in two CHF rabbits with iv infusion of the same dose of SIM (5μg/0.5μl/h for 7 days), we did not find alterations of baseline RSNA, baroreflex function, and nNOS protein expression in the RVLM (data not shown).

RhoA/ROCK pathway mediates the SIM induced up regulation of nNOS expression

In this experiment, we employed the CATH.a neuronal cell line to explore the mechanisms mediating SIM's effect on nNOS expression. We first observed the effects of three doses of SIM (0.1, 1, and 10 μM) on the nNOS mRNA expression. We found that 0.1 and 1 μM SIM significantly up regulated nNOS mRNA expression, but 10 mM SIM had no effect compared with the vehicle treatment (nNOS/GAPDH: 0.20 ± 0.09 in control, 0.52 ± 0.11 at 0.1 μM, 0.59 ± 0.12 at 1 μM, and 0.18 ± 0.07 in 10 μM SIM; $P < 0.05$). We also determined the time course of 1 μM SIM induced nNOS mRNA expression, demonstrating that 48, 72, and 96 hour treatment of SIM significantly up regulated nNOS mRNA expression and 24 hour treatment only exhibited a tendency to increase the nNOS mRNA expression but did not reach the statistical significance compared with control (nNOS/GAPDH: 0.10 ± 0.09 in control, 0.38 ± 0.11 in 24 h, 0.71 ± 0.14 in 48 h, 0.52 ± 0.10 in 48 h, and 0.47 ± 0.14 in 96 h SIM treatment; $P < 0.05$).

Figure 6 shows the effects of the HMG-CoA reductase products on the SIM induced up regulation of nNOS mRNA expression in CATH.a neurons. 1μM SIM incubation for 48 h significantly up regulated nNOS mRNA expression, which was completely abolished by the L-mevalonate (Mev, 200μm), Farnesylpyrophosphate (FPP, 5μm), and

geranylgeranylpyrophosphate (GGPP, 5μm). On the other hand, the inhibitor of Rho-associated kinase (ROCK), Y-27632 (100 μm), significantly up regulated nNOS mRNA expression.

Discussion

Our previous studies have demonstrated that oral treatment with SIM normalized sympathetic outflow and restored arterial baroreflex function in rabbits with pacing induced CHF via an inhibition of Angiotensin II mechanisms and reactive oxygen species in the RVLM(Gao, et al., 2005a; Pliquett, et al., 2003). In the current study, we further found that direct icv infusion of SIM also exhibited a beneficial effect on sympathetic nerve activity and baroreflex function in the CHF state. This was accompanied by an up regulation of nNOS protein expression in the RVLM. Moreover, icv co-infusion of SIM and L-NAME, completely abolished the effect of SIM on sympathetic nerve activity and baroreflex function but had no effects on nNOS expression. These results strongly suggest that increased central NO production is another critical pathway to normalize sympathetic nerve activity in the CHF state, and the elevated NO production at least partially resulted from the upregulation of nNOS expression in the RVLM.

As indicated above, NOS and NO in the RVLM have a major influence on sympathetic nerve activity in both physiological and pathological states. Vincent and Kimura(Vincent and Kimura, 1992) first demonstrated the presence of NOS-immunoreactive neurons in the RVLM of rats, which was further confirmed by Ohta et al.(Ohta, et al., 1993) and Simonian et al. (Simonian and Herbison, 1996). This morphological evidence implies a potentially functional involvement of RVLM local NO in the regulation of sympathetic outflow. Indeed, microinjection of sodium nitroprusside, a donor of NO, or L-arginine, a precursor for NO, into the RVLM of normal cats induced a reduction in RSNA and MAP(Shapoval, et al., 1991). In anesthetized rats microinjections of NO donors and NOS inhibitors into the RVLM exhibited sympatho-inhibitory and sympatho-excitatory effects respectively(Zanzinger, et al., 1995). In the current experiment, we found that icv infusion of SIM up regulated nNOS protein expression in the RVLM of CHF rabbits and the simultaneously decreased RSNA, suggesting that SIM induced suppression of sympathetic outflow was mediated, at least partially, by the NO/nNOS pathway. Indeed, the NOS inhibitor, L-NAME, abolished the effects of SIM on sympathetic nerve activity when co-infused with SIM, providing further evidence demonstrating the potential involvement of NO in this SIM effect. Moreover, functional data from this experiment shows that the SIM induced decrease in sympathetic nerve activity presented as early as day 2 post treatment and was sustained up to day 7 post SIM treatment. This was paralleled by an up regulated nNOS protein expression at day 2 and day 7 post SIM treatment. Recently, Kishi et al.(Kishi, et al., 2001) reported that gene transfer induced over expression of eNOS in the bilateral RVLM significantly decreased AP, HR, and sympathetic nerve activity in conscious rats, providing a more direct involvement of the RVLM NOS expression in the regulation of sympathetic outflow. They further demonstrated that eNOS over expression induced inhibition of sympathetic activity was mediated by an increased release of GABA in the RVLM. However, using Antibodies from the BD Biosciences, we did not detect the iNOS and eNOS protein expressions in the RVLM of rabbits in this current experiment (data not shown).

Another novel finding in this experiment is that icv infusion of SIM improved arterial baroreflex function of CHF rabbits. This may also be mediated by the NO/nNOS pathway in the RVLM since it was reversed by L-NAME treatment. Indeed, over expression of eNOS or nNOS by gene transfer into the RVLM has been demonstrated to improve the impaired arterial baroreflex function in either spontaneously hypertensive rats(Kishi, et al., 2003) or CHF rats (Wang, et al., 2003). We therefore postulated that SIM would suppress sympathetic nerve activity and the improved arterial baroreflex function. Based on the known effects of statins

we hypothesized that both of these effects would be due to up regulation of nNOS expression in the RVLM. It is well documented that sympathetic nerve activity and arterial baroreflex function are tightly interdependent. That is, activation of the arterial baroreflex markedly inhibits sympathetic outflow and sympathetic overactivity impairs baroreflex function. However based on the current experiments it is difficult to determine which whether these are two independent processes following treatment with SIM in CHF rabbits. When comparing the data in Figure 2 and 4, we noted that the slope of the baroreflex was gradually increased from day 1 to day 7 post SIM treatment with the peak at day 7. However, the basal RSNA appears to be decreased to the same degree from day 3 to day 7 after SIM treatment. Moreover, at day 2 and day 3, the basal RSNA in the SIM treated rabbits was lower than both before SIM treatment and vehicle treatment rabbits (Figure 2), however this was not the case for the arterial baroreflex (Figure 4). We therefore tend to regard the SIM induced inhibition of sympathetic activity as the cause of the SIM induced improvement in baroreflex function. Based on these data we believe that the critical sequences of events following SIM treatment are as follows: SIM up regulates nNOS expression in the RVLM, then suppresses sympathetic nerve activity which in turn improves arterial baroreflex function.

One critical question raised from the above results is how SIM upregulates nNOS expression. Statins, including SIM, are potent inhibitors of 3-hydroxy-3-methylglutaryl coenzyme A (HMG-CoA) reductase and cholesterol biosynthesis, and therefore are widely used in the treatment of hypercholesterolemia to prevent cardiovascular diseases such as myocardial infarction, stroke, and sudden cardiac death(Takemoto and Liao, 2001;Maron, et al., 2000). Recent evidence indicates that, statins also benefit the cardiovascular system via cholesterol-independent effects, including the inhibition of small GTP-binding protein Rho(Liao, 2002). The Rho-associated kinases (ROCKs) were found to be one of the first downstream targets of RohA(Matsui, et al., 1996;Leung, et al., 1995;Ishizaki, et al., 1996). In endothelial cells, statins induced inhibition of RhoA geranylgeranylation decreases membrane GTP-bound active RhoA and subsequent ROCK activity, leading to the up regulation of eNOS(Laufs and Liao, 1998). We therefore hypothesized that the same intracellular signaling pathway might also mediate the SIM induced up regulation of nNOS in neurons and observed the effects of exogenous isoprenoid intermediates on the SIM induced over expression of nNOS mRNA in CATH.a neurons. As was shown in Figure 6, the up regulation of nNOS mRNA expression by SIM treatment was completely abolished by the L-Mevalonate, Farnesyl-PP, and Geranylgeranyl-PP. These results suggest that the up regulation of nNOS by SIM appears to be specific to the inhibition of HMG-CoA reductase, as the addition of Mevalonate and its downstream products completely abolish the stimulatory effect of SIM on nNOS expression. Recently, Nakata *et al* (Nakata, et al., 2007) demonstrated that in cultured rat aortic smooth muscle cells, treatment with atorvastatin significantly increased nNOS mRNA and protein expression through the activation of the Akt/NF-κB pathway. It is not known if this pathway also mediated the SIM induced up regulation of nNOS mRNA expression observed in the current experiment. However, the time course of atorvastatin induced nNOS expression in smooth muscle cells is almost exactly the same as that of SIM induced nNOS expression in CATH.a cells with the initial increase in nNOS expression at day 1 and the peak effect at day 2 implying a potential common intracellular signaling pathway mediating the statin induced up regulation of nNOS in smooth muscle cells and neurons.

In conclusion, we demonstrated that centrally administered SIM decreased RSNA and improved arterial baroreflex function via up regulation of nNOS expression in the RVLM of CHF rabbits. We further documented that the inhibition of HMG-CoA reductase and its downstream pathway mediated the up regulation of nNOS by SIM, in which the RhoA/ROCK pathway plays a role.

Acknowledgements

Abbreviations

Mev

Mevalonate

FPP

Farnesyl-pyrophosphate

GGPP

geranylgeranyl-pyrophosphate

dbcAMP

N 6,2′-O-dibutyryladenosine 3′,5′-cyclemonophosphate

L-NAME

N_ω-Nitro-L-arginine methyl ester

References

Bredt DS, Hwang PM, Snyder SH. Localization of nitric oxide synthase indicating a neural role for nitric oxide. Nature 1990;347:768–770. [PubMed: 1700301]

Chan JY, Wang LL, Chao YM, Chan SH. Downregulation of basal iNOS at the rostral ventrolateral medulla is innate in SHR. Hypertension 2003;41:563–570. [PubMed: 12623960]

Chan JY, Wang LL, Wu KL, Chan SH. Reduced functional expression and molecular synthesis of inducible nitric oxide synthase in rostral ventrolateral medulla of spontaneously hypertensive rats. Circulation 2001;104:1676–1681. [PubMed: 11581148]

Dampney RA. The subretrofacial vasomotor nucleus: anatomical, chemical and pharmacological properties and role in cardiovascular regulation. Prog Neurobiol 1994;42:197–227. [PubMed: 8008825]

Di Napoli P, Antonio TA, Grilli A, Spina R, Felaco M, Barsotti A, De Caterina R. Simvastatin reduces reperfusion injury by modulating nitric oxide synthase expression: an ex vivo study in isolated working rat hearts. Cardiovasc Res 2001;51:283–293. [PubMed: 11470468]

DiBona GF, Sawin LL. Increased renal nerve activity in cardiac failure: arterial vs. cardiac baroreflex impairment. Am J Physiol 1995;268:R112–R116. [PubMed: 7840310]

Gao L, Wang W, Li YL, Schultz HD, Liu D, Cornish KG, Zucker IH. Simvastatin therapy normalizes sympathetic neural control in experimental heart failure: roles of angiotensin II type 1 receptors and NAD(P)H oxidase. Circulation 2005a;112:1763–1770. [PubMed: 16157767]

Gao L, Wang W, Li YL, Schultz HD, Liu D, Cornish KG, Zucker IH. Sympathoexcitation by central ANG II: roles for AT1 receptor upregulation and NAD(P)H oxidase in RVLM. Am J Physiol Heart Circ Physiol 2005b;288:H2271–H2279. [PubMed: 15637113]

Guertzenstein PG, Silver A. Fall in blood pressure produced from discrete regions of the ventral surface of the medulla by glycine and lesions. J Physiol 1974;242:489–503. [PubMed: 4455831]

Hirooka Y, Shigematsu H, Kishi T, Kimura Y, Ueta Y, Takeshita A. Reduced nitric oxide synthase in the brainstem contributes to enhanced sympathetic drive in rats with heart failure. J Cardiovasc Pharmacol 2003;42 Suppl 1:S111–S115. [PubMed: 14871040]

Ishizaki T, Maekawa M, Fujisawa K, Okawa K, Iwamatsu A, Fujita A, Watanabe N, Saito Y, Kakizuka A, Morii N, Narumiya S. The small GTP-binding protein Rho binds to and activates a 160 kDa Ser/

Thr protein kinase homologous to myotonic dystrophy kinase. EMBO J 1996;15:1885–1893. [PubMed: 8617235]

Kagiyama S, Tsuchihashi T, Abe I, Fujishima M. Cardiovascular effects of nitric oxide in the rostral ventrolateral medulla of rats. Brain Res 1997;757:155–158. [PubMed: 9200511]

Kishi T, Hirooka Y, Ito K, Sakai K, Shimokawa H, Takeshita A. Cardiovascular effects of overexpression of endothelial nitric oxide synthase in the rostral ventrolateral medulla in stroke-prone spontaneously hypertensive rats. Hypertension 2002;39:264–268. [PubMed: 11847195]

Kishi T, Hirooka Y, Kimura Y, Sakai K, Ito K, Shimokawa H, Takeshita A. Overexpression of eNOS in RVLM improves impaired baroreflex control of heart rate in SHRSP. Rostral ventrolateral medulla. Stroke-prone spontaneously hypertensive rats. Hypertension 2003;41:255–260. [PubMed: 12574091]

Kishi T, Hirooka Y, Sakai K, Shigematsu H, Shimokawa H, Takeshita A. Overexpression of eNOS in the RVLM causes hypotension and bradycardia via GABA release. Hypertension 2001;38:896–901. [PubMed: 11641305]

Krukoff TL. Central actions of nitric oxide in regulation of autonomic functions. Brain Res Brain Res Rev 1999;30:52–65. [PubMed: 10407125]

Laufs U, Liao JK. Post-transcriptional regulation of endothelial nitric oxide synthase mRNA stability by Rho GTPase. J Biol Chem 1998;273:24266–24271. [PubMed: 9727051]

Leung T, Manser E, Tan L, Lim L. A novel serine/threonine kinase binding the Ras-related RhoA GTPase which translocates the kinase to peripheral membranes. J Biol Chem 1995;270:29051–29054. [PubMed: 7493923]

Liao JK. Isoprenoids as mediators of the biological effects of statins. J Clin Invest 2002;110:285–288. [PubMed: 12163444]

Liu JL, Zucker IH. Regulation of sympathetic nerve activity in heart failure: a role for nitric oxide and angiotensin II. Circ Res 1999;84:417–423. [PubMed: 10066676]

Maron DJ, Fazio S, Linton MF. Current perspectives on statins. Circulation 2000;101:207–213. [PubMed: 10637210]

Matsui T, Amano M, Yamamoto T, Chihara K, Nakafuku M, Ito M, Nakano T, Okawa K, Iwamatsu A, Kaibuchi K. Rho-associated kinase, a novel serine/threonine kinase, as a putative target for small GTP binding protein Rho. EMBO J 1996;15:2208–2216. [PubMed: 8641286]

Nakata S, Tsutsui M, Shimokawa H, Yamashita T, Tanimoto A, Tasaki H, Ozumi K, Sabanai K, Morishita T, Suda O, Hirano H, Sasaguri Y, Nakashima Y, Yanagihara N. Statin treatment upregulates vascular neuronal nitric oxide synthase through Akt/NF-kappaB pathway. Arterioscler Thromb Vasc Biol 2007;27:92–98. [PubMed: 17082483]

Ohta A, Takagi H, Matsui T, Hamai Y, Iida S, Esumi H. Localization of nitric oxide synthase-immunoreactive neurons in the solitary nucleus and ventrolateral medulla oblongata of the rat: their relation to catecholaminergic neurons. Neurosci Lett 1993;158:33–35. [PubMed: 7694198]

Packer M. Pathophysiology of chronic heart failure. Lancet 1992;340:88–92. [PubMed: 1352022]

Pliquett RU, Cornish KG, Peuler JD, Zucker IH. Simvastatin normalizes autonomic neural control in experimental heart failure. Circulation 2003;107:2493–2498. [PubMed: 12695293]

Saheki A, Terasaki T, Tamai I, Tsuji A. In vivo and in vitro blood-brain barrier transport of 3-hydroxy-3-methylglutaryl coenzyme A (HMG-CoA) reductase inhibitors. Pharm Res 1994;11:305–311. [PubMed: 8165193]

Shapoval LN, Sagach VF, Pobegailo LS. Nitric oxide influences ventrolateral medullary mechanisms of vasomotor control in the cat. Neurosci Lett 1991;132:47–50. [PubMed: 1787918]

Simonian SX, Herbison AE. Localization of neuronal nitric oxide synthase-immunoreactivity within sub-populations of noradrenergic A1 and A2 neurons in the rat. Brain Res 1996;732:247–252. [PubMed: 8891292]

Takemoto M, Liao JK. Pleiotropic effects of 3-hydroxy-3-methylglutaryl coenzyme a reductase inhibitors. Arterioscler Thromb Vasc Biol 2001;21:1712–1719. [PubMed: 11701455]

Tseng CJ, Liu HY, Lin HC, Ger LP, Tung CS, Yen MH. Cardiovascular effects of nitric oxide in the brain stem nuclei of rats. Hypertension 1996;27:36–42. [PubMed: 8591885]

Vincent SR, Kimura H. Histochemical mapping of nitric oxide synthase in the rat brain. Neuroscience 1992;46:755–784. [PubMed: 1371855]

Wang Y, Patel KP, Cornish KG, Channon KM, Zucker IH. nNOS gene transfer to RVLM improves baroreflex function in rats with chronic heart failure. Am J Physiol Heart Circ Physiol 2003;285:H1660–H1667. [PubMed: 12969883]

Ye Y, Lin Y, Atar S, Huang MH, Perez-Polo JR, Uretsky BF, Birnbaum Y. Myocardial protection by pioglitazone, atorvastatin, and their combination: mechanisms and possible interactions. Am J Physiol Heart Circ Physiol 2006;291:H1158–H1169. [PubMed: 16603698]

Zanzinger J. Role of nitric oxide in the neural control of cardiovascular function. Cardiovasc Res 1999;43:639–649. [PubMed: 10690335]

Zanzinger J, Czachurski J, Seller H. Inhibition of basal and reflex-mediated sympathetic activity in the RVLM by nitric oxide. Am J Physiol 1995;268:R958–R962. [PubMed: 7733407]
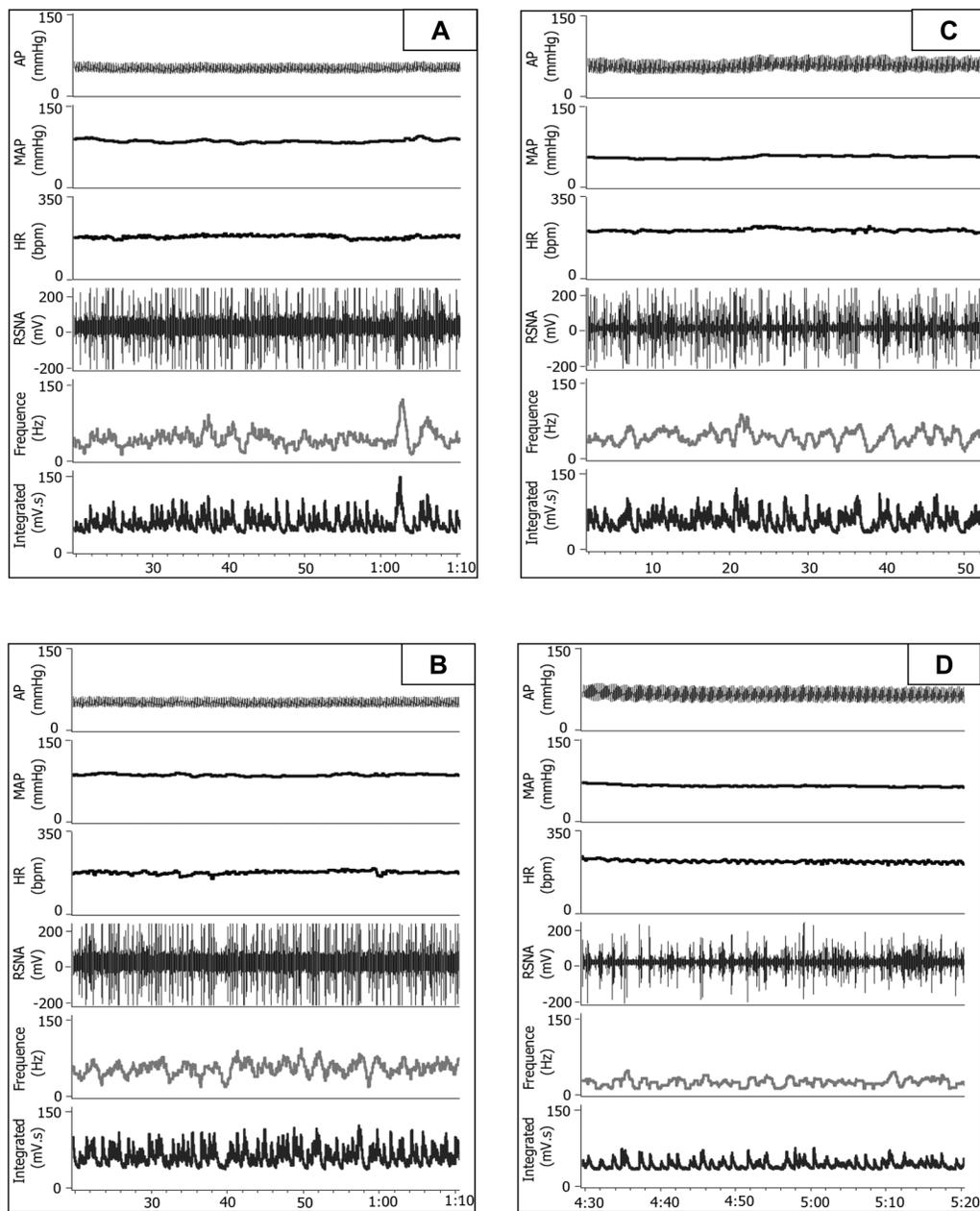
Figure 1.
Representative tracing from one vehicle (A and B) and one SIM (C and D) treated CHF rabbit showing basal blood pressure, heart rate, and renal sympathetic nerve activity pre treatment (A and C) and at the day 7 post treatment (B and D).
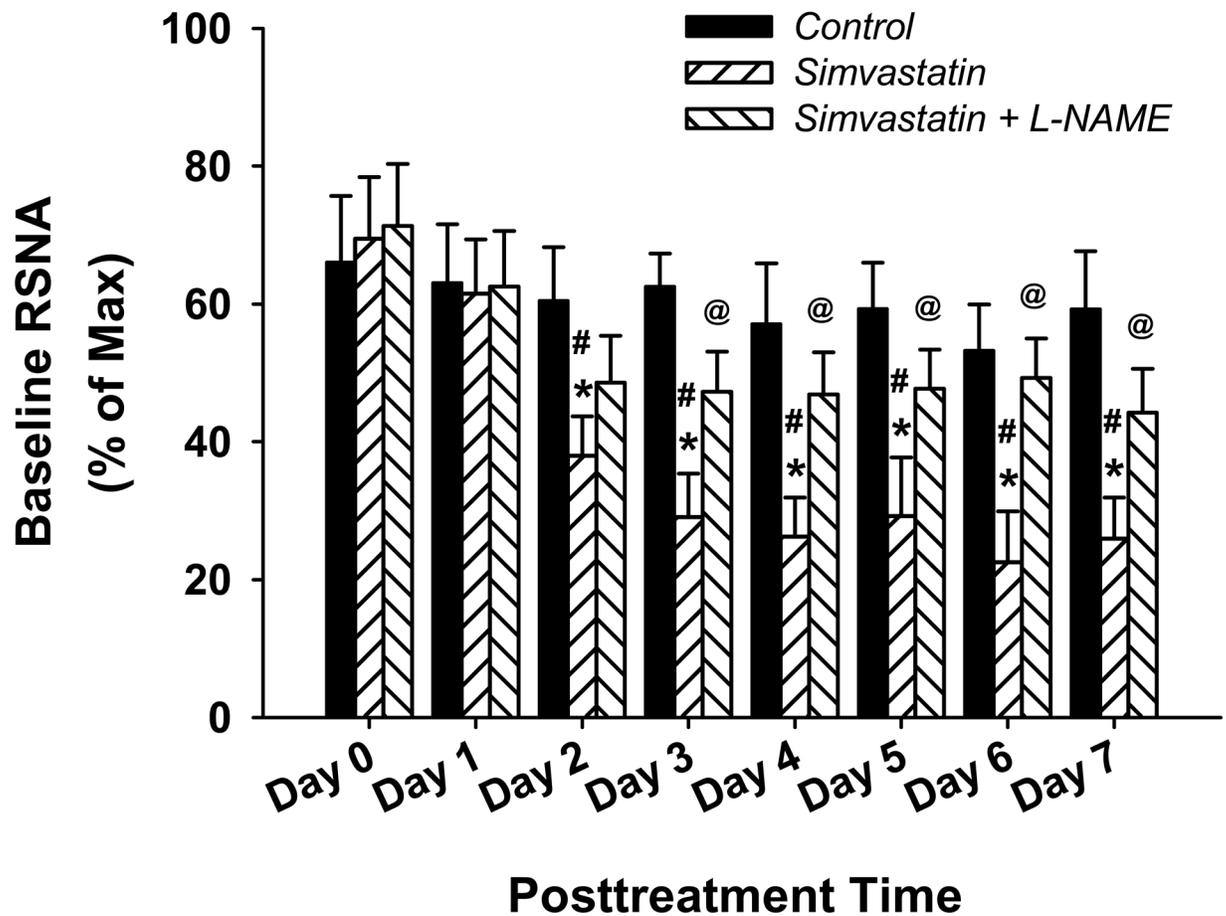
Figure 2.
Group data showing the time course of icv infusion of SIM induced decrease in renal sympathetic nerve activity, and blockade by L-NAME. $*P < 0.05$ compared with vehicle group; $^{\#}P < 0.05$ compared with before SIM treatment in the same group; $^{@}P < 0.05$ compared with SIM group. n = 6 in vehicle group, 7 in SIM group, 5 in SIM + L-NAME group.
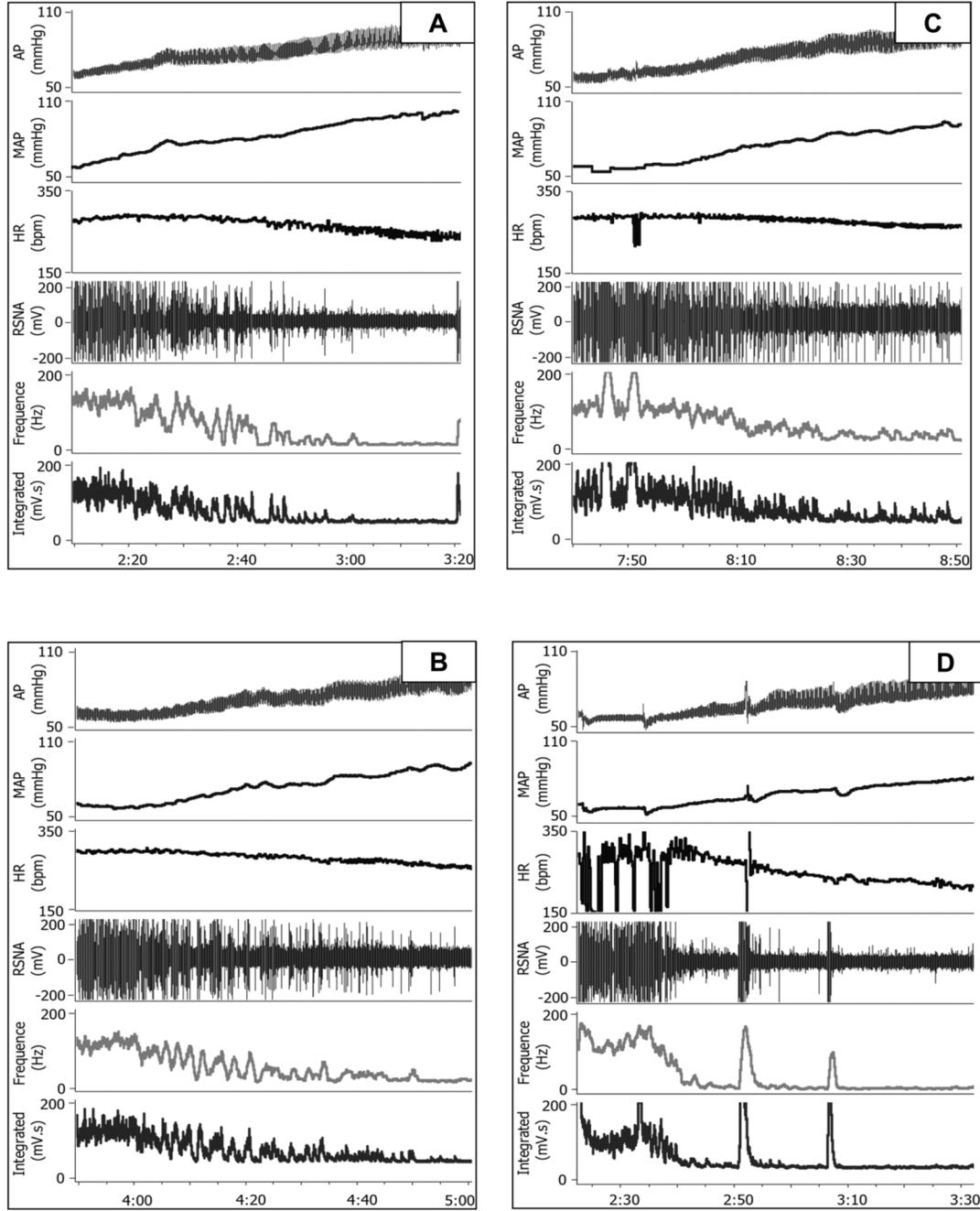
Figure 3.
Original recording of arterial blood pressure changes induced by iv infusion of phenylephrine and attendant reflex RSNA and HR responses before (A and C) and after (B and D) vehicle (A and B) and SIM (C and D) treatment in the CHF rabbits. Note the improved reflex sympatho-inhibition and bradycardia responses to the phenylephrine induced pressor effect after SIM treatment (D) compared with either before SIM treatment (D) or vehicle treatment (B).
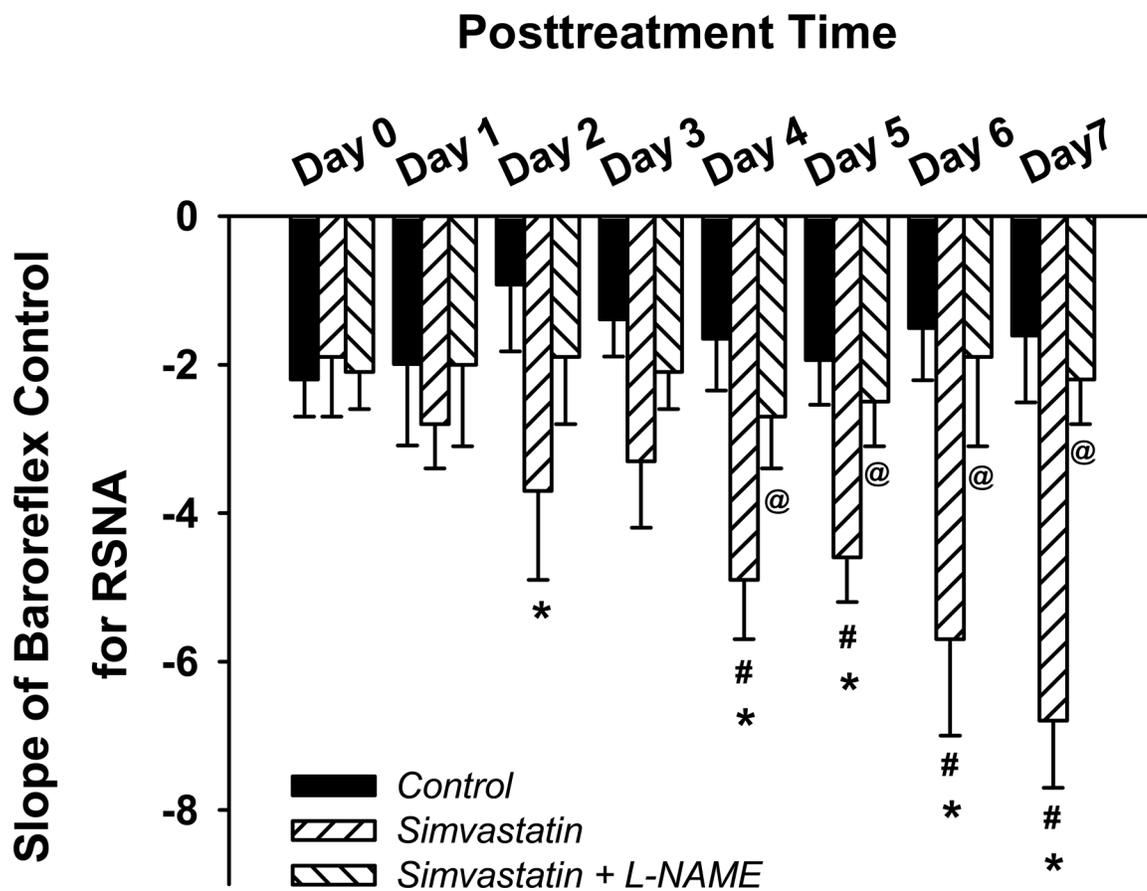
Figure 4.
Group data showing the time course of icv infusion of SIM induced increase in the arterial baroreflex function, and the blockade of L-NAME on this SIM effect. *$P < 0.05$ compared with vehicle group; #$P < 0.05$ compared with before SIM treatment in the same group; @$P < 0.05$ compared with SIM group. n = 6 in vehicle group, 7 in SIM group, 5 in SIM + L-NAME group.
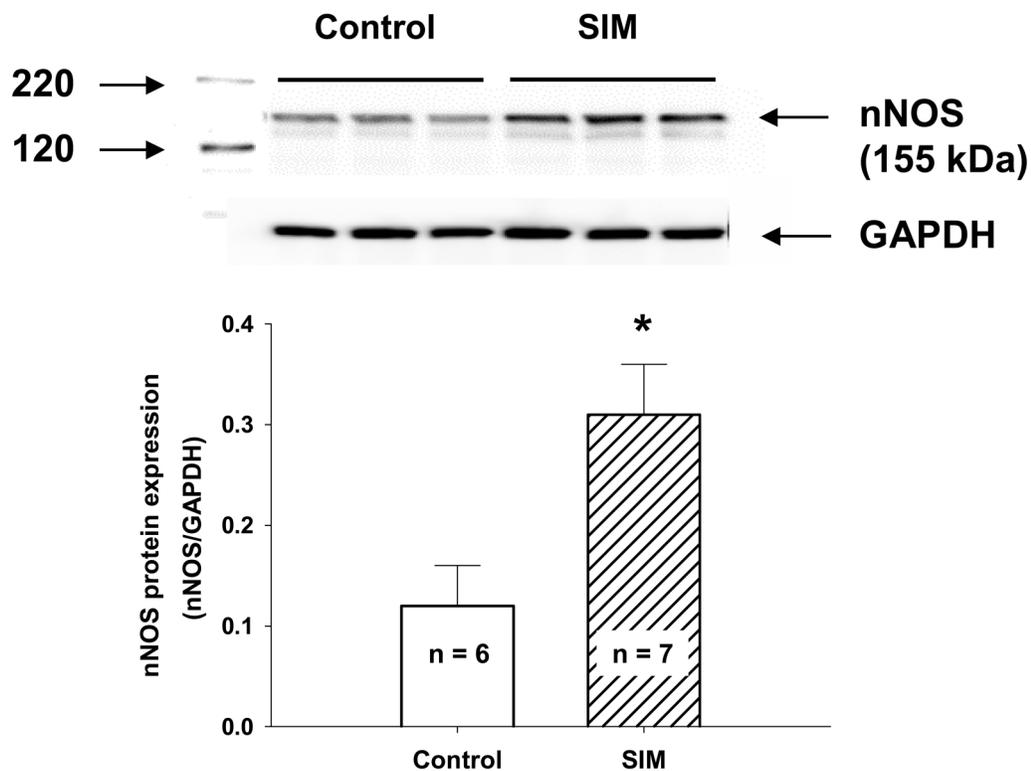
Figure 5.
Western blot analysis for protein expression of nNOS in the RVLM. *Top panel*: representative Western blots showing the up regulation of nNOS protein expression in the RVLM of a SIM treated CHF rabbit compared with a vehicle treated CHF rabbit. *Bottom panel*: results of densitometric analysis representing means ± SE. *$P < 0.05$ compared with vehicle group.
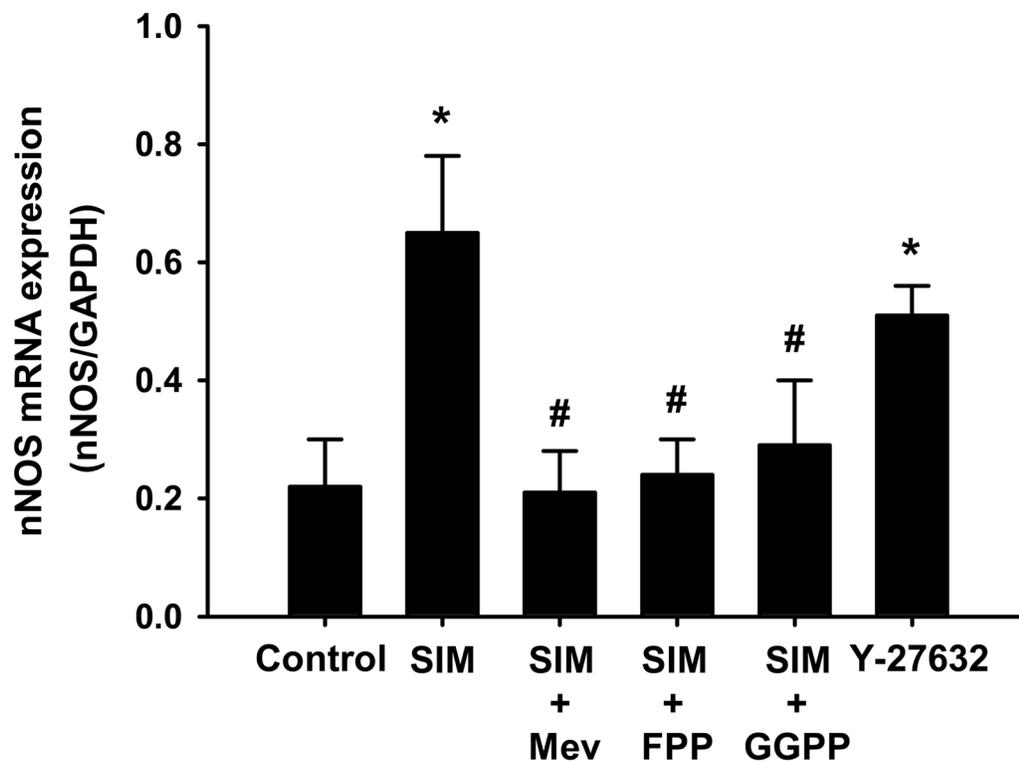
Figure 6.
Real-time RT-PCR analysis for mRNA expression of nNOS in the CATH.a neuronal cell line.
SIM: Simvastatin; Mev: L-Mevalonate; FPP: farnesyl-pyrophosphate; GGPP: geranylgeranyl-pyrophosphate; Y-27632: inhibitor of ROCK. *$P < 0.05$ compared with vehicle group. #$P < 0.05$ compared with SIM group. n = 4.

Table 1

Gene-specific primers and probes for real-time RT-PCR used in this experiment.

Name of genes (Accession No.)	Forward primers	Reverse primers	Probes	Amplicon
Mouse nNOS (AK141904)	ATCACAGGCAC AAATGGAGA	TGATCCACTGCC TGGTTAAA	TGGGTCCTCCACA GGGACCC	123
Mouse GAPDH (NM_001001303)	ACAACTTTGGCA TTGTGGAA	GATGCAGGGAT GATGTTCTG	CATGCCATCACTG CCACCCA	133

*
nt, nucleotide numbers.

Table 2

Baseline data in the three group rabbits

	Vehicle		Simvastatin		Simvastatin + L-NAME	
n	6		7		5	
	Before	After	Before	After	Before	After
BW, kg	-	3.9 ± 0.4	-	3.6 ± 0.3	-	4.1 ± 0.3
HW/BW, g/kg	-	3.4 ± 0.3	-	3.5 ± 0.5	-	3.2 ± 0.3
LW/BW, g/kg	-	5.4 ± 0.3	-	5.1 ± 0.4	-	4.9 ± 0.5
MAP, mm Hg	70.6 ± 3.4	73.2 ± 5.9	73.7 ± 5.5	74.5 ± 4.2	72.7 ± 6.1	74.1 ± 4.6
HR, bpm	227.9 ± 7.5	241.3 ± 10.2	246.2 ± 6.9	232.9 ± 11.8	231.7 ± 9.4	239.5 ± 8.4
LVEDP, mm Hg	-	15.4 ± 2.2	-	14.4 ± 2.5	-	14.9 ± 2.6
LVEDD, mm	-	18.8 ± 0.9	-	17.6 ± 0.7	-	17.9 ± 0.8
EF, %	36.3 ± 4.1	34.6 ± 5.3	37.8 ± 5.4	39.2 ± 4.1	36.6 ± 5.3	37.6 ± 4.3

Values are means ± SE. Before: before treatment; After: at day 7 after treatment; *n*, no. of animals; BW, body weight; HW, heart weight; LW, lung weight; MAP, mean arterial pressure; HR, heart rate; LVEDD, left ventricular end-diastolic diameter; LVEDP, left ventricular end-diastolic pressure; EF, ejection fraction.